Available online at www.sciencedirect.com
SCIENCE DIRECT
ELSEVIER
Journal of the European Ceramic Society 26 (2006) 993–1001
ECERS
www.elsevier.com/locate/jeurceramsoc

Preparation and experimental characterization of glass–alumina functionally graded materials

V. Cannillo, T. Manfredini, C. Siligardi*, A. Sola

Dipartimento di Ingegneria dei Materiali e dell'Ambiente, University of Modena and Reggio Emilia, Via Vignolese 905, 41100 Modena, Italy

Received 2 September 2004; received in revised form 2 December 2004; accepted 10 December 2004
Available online 5 February 2005

Abstract

This work aims at investigating the effects of the processing conditions on the final microstructure of glass–alumina functionally graded materials (FGMs). The ingredient materials, i.e. a polycrystalline sintered alumina and a $CaO–ZrO_2–SiO_2$ glass, were accurately characterized, since their mechanical and thermal properties may deeply influence the fabricating process and the overall FGM behaviour. The functionally graded materials were obtained by means of percolation of the molten glass into the alumina substrate. Two types of samples were considered—the "Bulk" FGMs, produced starting from a glass bulk, and the "Powder" FGMs, produced starting from a glass powder; in both cases four different heating cycles were attempted. The functionally graded materials were analysed using a SEM-EDS and a X-ray diffractometer. Great attention was devoted to the resulting microstructure; moreover the depth of penetration was measured and related to the fabricating parameters, such as time and temperature.

Keywords: Al_2O_3; Glass; FGM; Microstructure-final

1. Introduction

Functionally graded materials are special composite materials whose composition and microstructure are not uniform in space, but gradually vary following a predetermined law. These materials were first introduced as high performance thermal barrier coatings, but nowadays they are widely used in many fields, such as aerospace, microelectronics and biomedical engineering. Functionally graded materials owe their success to two main features. First of all, the gradual change in composition allows to exploit the constituent phase properties but, unlike traditional bi-materials junctions, it avoids the abrupt coupling of heterogeneous phases. Moreover the functional gradient can be tailored to the application requirements, even if the thermo-mechanical loading conditions are different from point to point. FGMs, therefore, imply a new approach to component design, since material property gradation and device configuration are engineered together.[1,2]

In the past, functionally graded materials composition typically included at least one metal phase.[2,3] Recently, however, great attention has been devoted to ceramics–ceramics and glass–ceramics systems, due to their attractive properties. Giannakopoulos et al., for example, produced convincing experimental and computational evidence of the potentiality of glass–alumina functionally graded materials.[4,5] They fabricated the FGM samples starting from a polycrystalline sintered alumina and a ternary glass belonging to the system $CaO–Al_2O_3–SiO_2$. After melting, the glass percolated into the alumina substrate and created a gradual change in composition along the penetration direction. The corresponding variation in mechanical properties resulted in innovative performances, such as the suppression of Hertzian-cone cracking.[4] In a second paper concerning the same alumina–glass system, Suresh et al. demonstrated that the controlled gradient in elastic modulus can result in a pronounced enhancement in the superficial resistance to frictional sliding contact.[5] Finally, Cannillo et al. further devel-

* Corresponding author. Tel.: +39 059 378416; fax: +39 059 373643.
E-mail address: siligardi@unimo.it (C. Siligardi).

0955-2219/$ – see front matter © 2005 Elsevier Ltd. All rights reserved.
doi:10.1016/j.jeurceramsoc.2004.12.017

oped a computational approach to investigate glass–alumina FGMs, showing that the overall behaviour is deeply influenced by the actual distribution of the constituent phases.[6,7]

Since the final composition and microstructure are determined by the fabricating process, it would be desirable to gain a deeper insight into the relation existing between fabricating parameters and microstructural features which, in turn, govern the FGM behaviour. This work, therefore, focused on glass–alumina functionally graded materials and inquired closely the effect of production conditions on the resulting microstructure.

Instead of an alumino-silicate glass, a glass belonging to the $CaO–ZrO_2–SiO_2$ ternary system was chosen. Besides showing good chemical, physical and mechanical properties,[8] the glasses belonging to this system do not contain any aluminium oxide, which is the only constituent of the substrate, and this makes easier the experimental investigation of the FGM samples. Moreover the glass composition was purposely designed in order to achieve a coefficient of thermal expansion quite similar to that of the alumina. The minimization of the mismatch in thermal properties may be advantageous to the FGM performance, by sensibly reducing the thermal residual stresses which may arise in service or during fabrication.[9]

The glass infiltration was induced by means of a thermal treatment. In spite of the simplicity of the applied fabricating procedure, many parameters could be changed, such as the time and temperature of the soaking step or the initial state—powder or bulk—of the glass. The resulting glass–alumina functionally graded materials were carefully characterized, with the intention of understanding the effects of processing on microstructure.

2. Experimental procedure

2.1. Ingredient materials preparation

The substrate was made up of an industrial high purity (99%), sintered alumina.[10] The alumina was supplied in the form of 60 mm wide square tiles, which were cut into smaller pieces of about 10 mm × 8 mm × 25 mm. Table 1 briefly summarises the most important alumina properties declared by the manufacturers. As already mentioned, for the glass phase a composition belonging to the $CaO–ZrO_2–SiO_2$ system was chosen. The molar oxide percentages of the glass composition are as follows: CaO 33.78%; ZrO_2 8.69%; SiO_2 57.53%. The raw materials were industrial powders, commonly used in the production of ceramic frits: quartz (Sikron 300 Colorobbia Italia); calcium carbonate (Colorobbia Italia); zirconium silicate (Zircobit FU, Colorobbia Italia). The powders were weighted and dry mixed for 40 min; the glass was melted in a platinum crucible at 1550 °C for 1 h. Then some glass was poured into proper graphitic moulds, thus obtaining a bar and a disk; the remaining glass was plunged into cold water, in order to make a frit. The glass looked perfectly homogeneous in the molten state. The bar and disk were annealed at 810 °C for 1 h and then slowly cooled down to room temperature. The bar was cut into 1.0 mm thick slices, while the disk was polished, resulting in a regular cylinder useful for the measurement of elastic properties by means of a resonance technique. The frit, in turn, was wet ball-milled, sieved through a 32 μm-meshed sieve and dried off in a kiln.

Table 1
Alumina properties declared by the manufacturers[9]

Property	Value
Density	3.86 g/cm^3
Young modulus	380 GPa
Vickers hardness, H_{V10}	14 GPa
Fracture toughness, K_{IC}	2.6 MPa m$^{1/2}$
Bending strength (4 points)	318 MPa

2.2. Functionally graded materials preparation

Some FGM samples were produced starting from the glass slices; others were fabricated using the glass powder. The former samples were named “Bulk” functionally graded materials, the latter ones “Powder” functionally graded materials. The same heating cycles were followed for both types of FGM samples.

As concerns the “Bulk” FGM samples, a glass slice was placed onto the top face of an alumina body and then heat treated. After melting, the glass penetrated into the polycrystalline substrate. Four different heat treatments were considered: in a typical cycle, the sample was heated from room temperature to 500 °C at 5 °C/min and then from 500 °C to 1500 °C at 10 °C/min; it was left at 1500 °C for 2 h; finally, the treatment closed with a cooling down from 1500 °C to 1000 °C at 10 °C/min and from 1000 °C to room temperature in air. The attempted heat treatment differed for the maximum temperature reached, which could be 1500 °C or 1600 °C, and for the length of the isothermal step, which could be 2 h or 4 h.

For the “Powder” samples, the glass powder was applied in the form of an aqueous suspension. The powder weight fraction was optimized in the attempt to improve the rheological properties, while minimizing the water content. A 66.5 wt.% of glass powder was found to be the best solution. The addition of a 2 wt.% vynilic binder was required in order to ensure the handiness of the glass–alumina green systems. A 0.6 mm thick layer of glass suspension was evenly distributed on each alumina substrate. After completely drying the water off in a kiln, the glass–alumina systems were heat treated in order to produce the functionally graded materials. The same four heat treatments were performed, as previously described with concern to the “Bulk” FGM samples.

2.3. Ingredient materials characterization

The data declared by the alumina manufacturers[10] were confirmed by the experimental analysis, whose procedure and results were described in an another work.[11]

The mechanical properties of the glass were measured by means of a resonance technique (EMOD, Lemmens Grindosonic® MK5) on the disk-shaped (5 cm diameter) sample, after properly polishing it. The coefficient of thermal expansion was measured with a NETSCH—DIL 404 dilatometer. In order to investigate the glass thermal behaviour, a differential thermal analysis (NETZSCH—DSC 404) was performed, heating the sample from room temperature to 1400 °C at 10 °C/min. The results of the glass DTA were described and discussed in a previous work.[8,12] However, the thermal treatment applied in order to evaluate the glass reactivity was relevantly different from the FGM fabricating process. Therefore, the previously described four FGM heat treatments were repeated on four glass slices. During the treatment, each glass slice was placed on a platinum plate, thus avoiding any reaction between the glass and the furnace refractory.

Finally, in order to measure the glass hardness and fracture toughness (K_{IC}), a glass fragment was suitably cut, embedded in unsaturated poly-ester resin and carefully polished. The Vickers microindentations (REMET HX-1000) were performed under three different loads, i.e. 25 g_f for 15 s, 50 g_f for 15 s and 100 g_f for 15 s. For each load, 25 tests were carried out. The permanent indents were observed under a scanning electron microscope (PHILIPS XL 40) and measured. As regards the toughness evaluation, 15 Vickers microindentations were performed under a load of 300 g_f for 15 s and the indents were observed and measured as well.

2.4. Functionally graded materials characterization

As concerns the "Bulk" samples, independently of the heat treatment applied, at the end of the thermal cycle some residual glass remained on the top surface of the FGM samples. Though the aforementioned reference glass slices were still amorphous after the heat treatment, in the "Bulk" FGMs the superabundant glass crystallized and broke off the substrate. Both the fracture surfaces—glass side and substrate side—looked completely crystallized. Therefore, for each sample, both the glass and the substrate delamination surfaces were observed under the SEM. The glass–air interface—i.e. the glass top surface—was studied as well. Finally, the cross-section of the bulk FGMs was observed using the SEM. Furthermore, in order to study the glass penetration into the alumina substrate and to evaluate the depth reached, the FGM cross-sections underwent a local chemical analysis by EDS. The molar percentages of the aluminium oxide and silicon oxide (assumed as a marker of the glass) were measured as a function of depth. The "Bulk" FGM sample investigation was completed by the X-ray diffraction analysis, which was performed on both the substrate cross-section and the superabundant glass top layer. As a matter of fact, the substrate sample was a bulk slice, while the superficial glass layer was finely ground.

Unlike the "Bulk" FGMs, the functionally graded materials produced starting from the glass powder ("Powder" FGMs) did not undergo any delamination and therefore the analysis was focused on the cross-section, which was characterized in the same way as the "Bulk" FGMs.

3. Results

3.1. Ingredient materials

As expected, the glass shows quite good mechanical properties[8]:

- Young modulus, $E = 90.56$ GPa.
- Shear modulus, $G = 35.50$ GPa.
- Poisson coefficient, $\nu = 0.28$.

The glass and the alumina Young moduli are quite different, but the Poisson coefficients are similar, which may be advantageous for the FGM resulting performance.[4]

The coefficients of thermal expansion are $8.06 \times 10^{-6}\ K^{-1}$ for the glass and $8.20 \times 10^{-6}\ K^{-1}$ for the alumina (Fig. 1). It is worth noting that the difference between the glass and the alumina coefficients of thermal expansion is really low in value. As already mentioned, a good compatibility between the thermal properties of the ingredient materials is a crucial requirement, since the mismatch in the coefficients of thermal expansion is likely to give rise to residual stresses which, in turn, may cause local damages and eventually cracks.[9]

The DTA results show that the glass transition occurs at about 800 °C. As described in previous works,[8,12] the exothermal peak at about 1000 °C may be due to the crystallization of wollastonite as main phase and a calcium zirconium silicate, $Ca_2ZrSi_4O_{12}$, as a secondary phase. Moreover, two endothermal peaks are visible: the first one, at about 1240 °C, is likely to be associated with the transformation of wollastonite into pseudo-wollastonite; the second one, at about 1360 °C, may be caused by the complete softening of the glass or by the melting of one of the aforementioned crystal phases.

It is worth noting that the reference glass slices do not undergo any crystallization process during the FGM heating cycles. As a matter of fact, independently of the heating

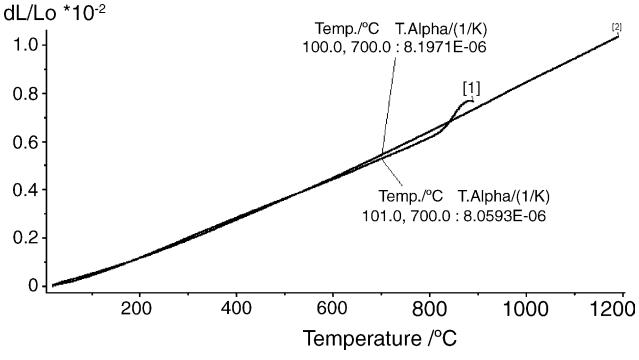

Fig. 1. Comparison between the glass [1] and the alumina [2] dilatometric curves. The coefficients of thermal expansion are really similar.

Table 2
Comparison between the calculated values of the glass fracture toughness

Equation	K_c (MPa m$^{1/2}$)
EC	1.32 ± 0.18
B	1.21 ± 0.09
JL	1.55 ± 0.22

schedule, all samples remain completely glassy. In order to justify the different glass behaviour, it should be noted that during the FGM production the heating conditions are not favourable to the glass crystallization. As a matter of fact, the differential thermal analysis suggests that the glass crystallization occurs at about 1000 °C, but in the FGM fabricating process the maximum temperature reached (1500 °C and 1600 °C, respectively) is so high that the glass system completely melts and, at the end of the quick cooling down step, the sample is abruptly extracted from the oven at about 1000 °C. As a consequence, the glass has not time enough to crystallize and remains totally amorphous.

The glass hardness, that can be deduced from the Vickers micro-indentations,[13] results:

$$H_{V30} = 693 \pm 39\,\text{kg/mm}^2 = 6.798 \pm 0.382\,\text{GPa}$$

The reliability of this value is confirmed by the analysis of the 25 g_f and 100 g_f indents. Then the K_{IC} value can be calculated according to three different equations: the Evans and Charles equation (named EC), the Blendell equation (B) and the Lankford equation (JL).[14] The results are listed in Table 2. The Evans and Charles equation returns a value which is intermediate between the Blendell and the Lankford ones, a result which is consistent with the analysis developed by Ponton and Rawlings.[15] In conclusion, the glass shows good mechanical properties and, in particular, the Vickers hardness and fracture toughness are relatively high in value. The glass performances are to be ascribed to the high content in zirconium oxide of the chosen composition.

3.2. *"Bulk" functionally graded materials*

As already mentioned, during the heat treatment some superabundant glass does not infiltrate the alumina (Fig. 2) and crystallises (Fig. 3). Since the reference glass slices remain amorphous, the glass crystallization in the "Bulk" FGM samples may be due to the alumina grains, which act as nucleating agents. Provided that the new crystal phases and the alumina substrate have different thermal properties, the thermal stresses, which arise during the heat treatment, may lead to the observed interfacial delamination.

The SEM-EDS investigation demonstrates that the four "Bulk" FGMs have analogous properties. When the glass side of the delamination surface is considered, three phases—a light grey matrix, a dark grey matrix, some white globular precipitates—can be seen. The EDS measurements reveal that the light grey areas contain silicon, calcium, zirconium and aluminium, whereas the dark grey domains contain silicon, calcium and aluminium, but the zirconium content is quite low. Finally, the white spherical bodies mainly contain zirconium. Their composition and their shape suggest that the white spherical bodies are originated by the precipitation of a zirconium oxide crystal phase. In order to identify the mineralogical phases, however, an X-ray analysis is required. Independently of the fabrication thermal cycle, the X-ray diffraction patterns of the glass top-layer show a wide broad band, due to the copious amorphous phase still present. Besides this, the most important crystal phase which can be identified is the anorthite ($CaAl_2Si_2O_8$), which confirms the aluminium diffusion into the glass. Furthermore, the crystallization of anorthite can justify the delamination of the top layer, since the anorthite coefficient of thermal expansion is noticeably lower than that of alumina (Table 3). Because of the mismatch in coefficients of thermal expansion, while cooling down the top layer contracts less quickly than the substrate and eventually spalls off. Finally, the X-ray diffraction analysis shows the presence of monoclinic zirconia.

When the delamination surface of the substrate is considered (Fig. 4), it is possible to distinguish the same three phases (light grey matrix; dark grey matrix; white spherical precipitates). According to the EDS analysis, their composition is the same as well.

The SEM observation of the substrate cross-section (Fig. 5) confirms that the glass penetrates into the polycrystalline alumina and the depth of penetration is greater in the samples which undergo the most severe thermal treatments. During the FGM heat treatment, some zirconium oxide crystals precipitate along the profile; the crystals are usually more

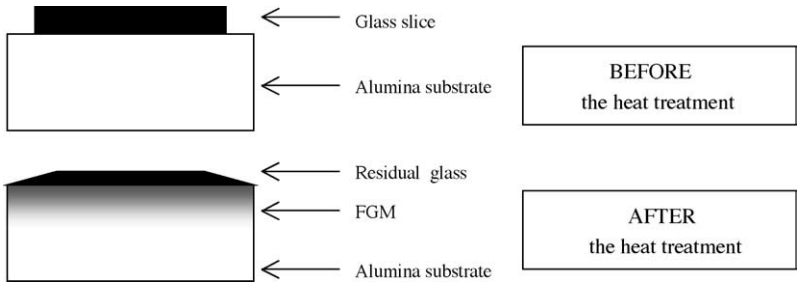

Fig. 2. Drawing illustrative of the incomplete glass penetration into the alumina substrate (not in scale); because of the thermal residual stresses, the superficial residual glass usually gets separated from the substrate.

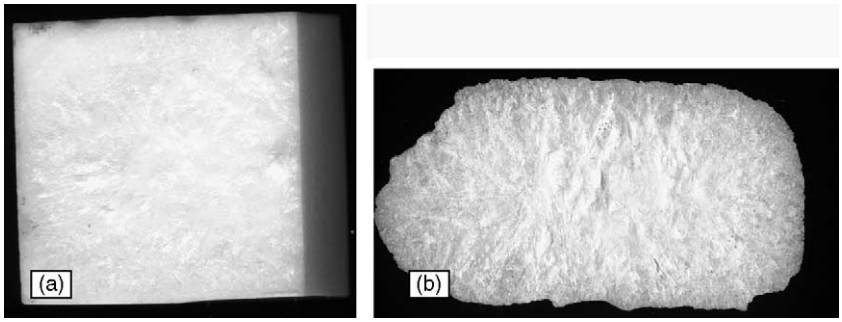

Fig. 3. Substrate (a) and superabundant glass (b) fracture surfaces. Both of them are completely crystallized.

Table 3
Comparison between the alumina and anorthite coefficients of thermal expansion

	CoeffIcient of thermal expansion (K^{-1})	Temperature range (°C)
Alumina	8.19×10^{-6}	20–1000
Anorthite	4.5×10^{-6} [18]	100–200[18]

abundant in the area next to the glass–substrate interface and preferentially grow between the alumina grains. This hints that the alumina grain boundaries stimulate the zirconium oxide crystallization kinetics. Nevertheless, according to the X-ray diffraction analysis, the α-alumina is the only crystal phase which can be detected in the substrate. This means that the amount of the zirconium oxide crystals is so low that it does not reach the instrumental threshold of detectability (1%). Therefore, it is reasonable to assume that the zirconium oxide crystals do not significantly influence the FGM overall behaviour.

In order to examine the resulting compositional gradient and the depth of penetration, the molar percentages of

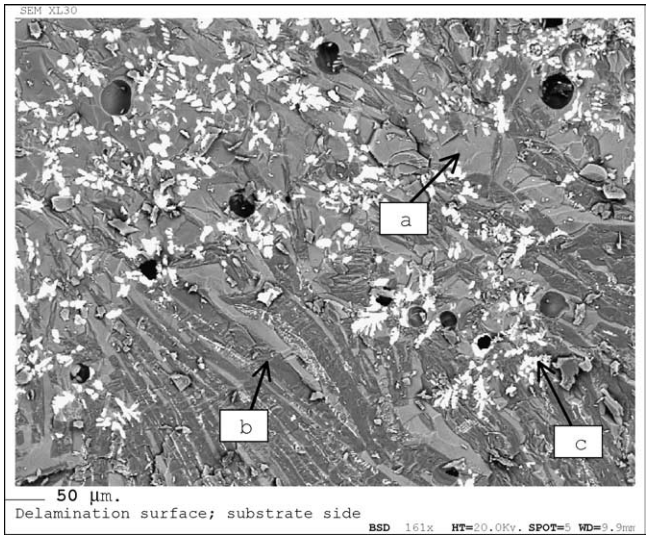

Fig. 4. The back-scattered electron (BSD) image clearly shows that in the "Bulk" FGMs three phases can be identified on the substrate delamination surface: a light grey matrix (a), a dark grey matrix (b) and some white bodies (c) (sample left at 1600 °C for 4 h).

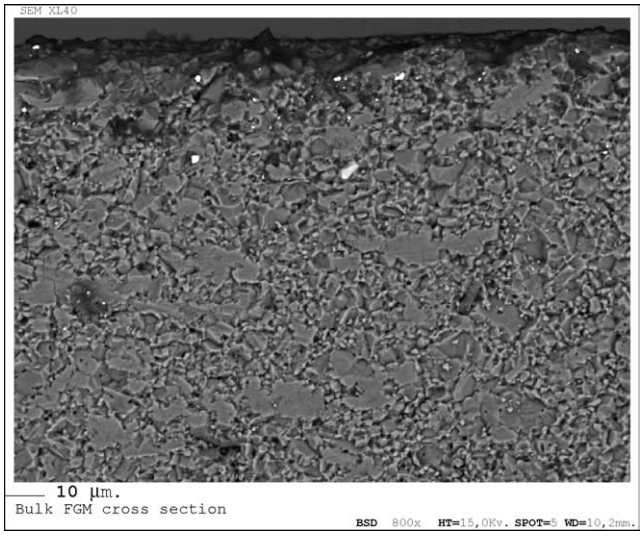

Fig. 5. Typical "Bulk" FGM cross-section (sample left at 1600 °C for 4 h).

the aluminium oxide and silicon oxide were measured as a function of depth. The experimental graphs, however, are not strictly monotonic, since the FGM microstructure is discrete and stochastic in nature,[6,7] while the measurement technique is punctual (Fig. 6). The curves, therefore, are just repre-

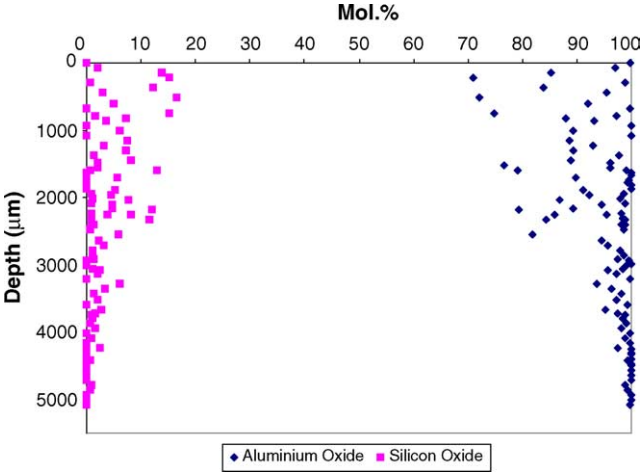

Fig. 6. EDS analysis of the bulk FGM heat-treated at 1600 °C for 4 h.

Table 4
Summary of the depths of penetration for different glass states and heating parameters

	"Bulk" FGMs (μm)	"Powder" FGMs (μm)
1500 °C, 2h	≈850	≈675
1500 °C, 4h	≈1600	≈1500
1600 °C, 2h	≈2800	≈2800
1600 °C, 4h	≈4400	≈5000

sentative of a trend and are useful to estimate the depth of penetration of the glass, measured where the silicon oxide molar fraction goes to zero. The depths of penetration result relevantly different for the four heat treatments attempted (Table 4).

3.3. "Powder" functionally graded materials

It is worth noting that, unlike the "Bulk" FGMs, the "Powder" samples do not undergo any delamination. However, the samples heat-treated at 1600 °C look quite deformed; in the samples treated for 2 h, the deformation mainly involves the upper part of the body (Fig. 7), while in the samples treated for 4 h the deformation affects the whole body. This phenomenon is much less evident in the samples treated at 1500 °C.

As already seen in the "Bulk" FGMs, the "Powder" FGMs show a superficial layer of superabundant glass (Fig. 8). Independently of the heating cycles, this glass, which can not penetrate into the substrate, undergoes a widespread crystallization and gives rise to a glass–ceramics coating, characterized by anorthite crystals and zirconia precipitates embedded in an amorphous matrix (Fig. 9). The glass–air interface is particularly rich in zirconia spherical precipitates, surrounded by a net of anorthite acicular crystals (Fig. 10).

The SEM-EDS analysis of the substrate confirms that the glass percolates along the alumina grain boundaries, seldom separating some zirconia crystals. Yet, independently of the heat treatment, the X-ray diffraction of the substrate cross-section detects the presence of only one crystal phase, that is to say the α-alumina of the substrate. It may be concluded, therefore, that also in the "Powder" FGMs the zirconium oxide crystal phase does not reach the threshold of detectability of the diffractometer.

The compositional profiles (Fig. 11), which were measured using the EDS, show that the depth of glass penetration depends on the heat treatment performed, as summarized in Table 4.

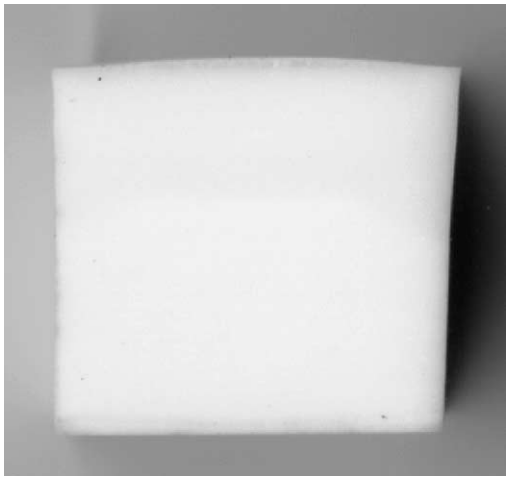

Fig. 7. The "Powder" FGM, left at 1600 °C for 2 h, shows an evident deformation in its upper part.

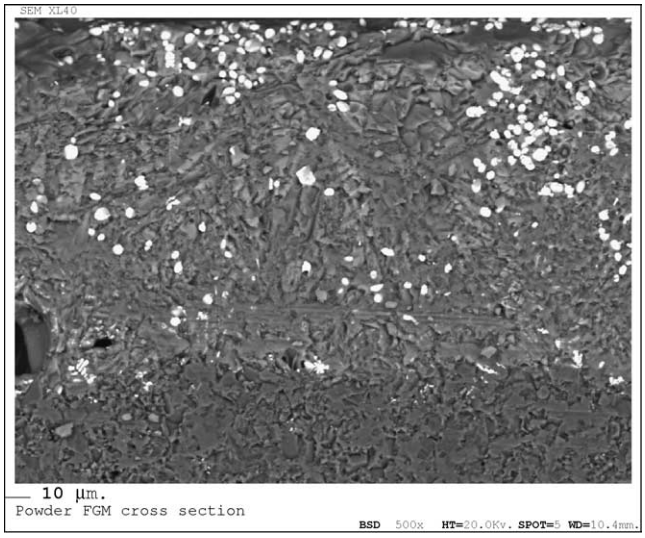

Fig. 8. Typical microstructure of a "Powder" FGM cross-section (sample left at 1600 °C for 4 h).

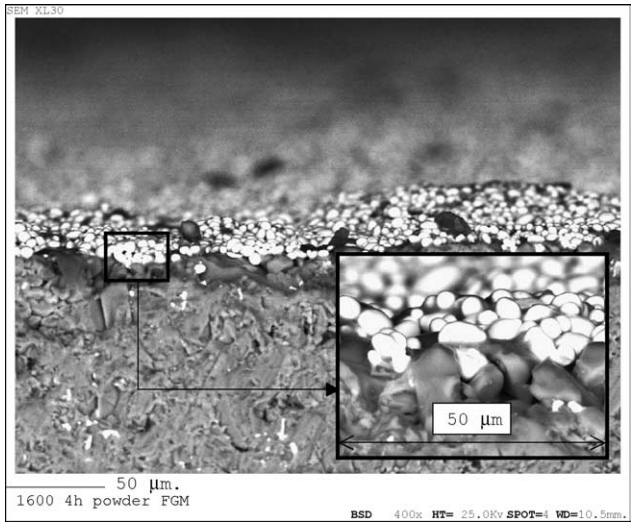

Fig. 9. In the "Powder" FGMs the glass which can not penetrate into the alumina substrate give rise to a glass–ceramics coating; the detail shows the zirconia spherical precipitates, particularly abundant on the surface (sample left at 1600 °C for 4 h).

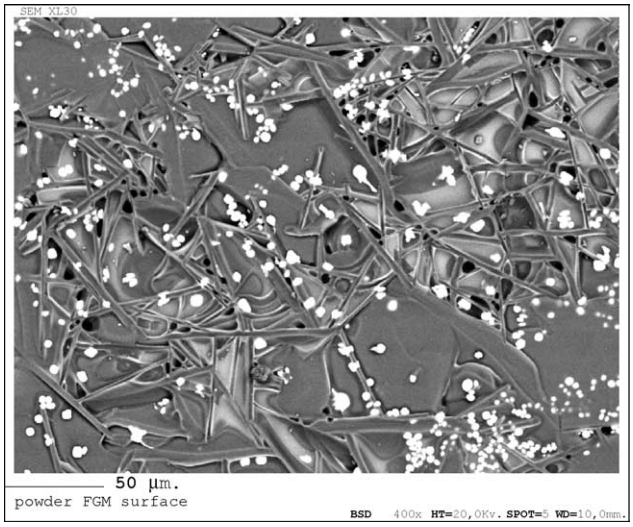

Fig. 10. In the "Powder" FGM samples, the glass–air interface is rich in zirconia spherical precipitates, surrounded by acicular anorthite crystals (sample left at 1600 °C for 4 h).

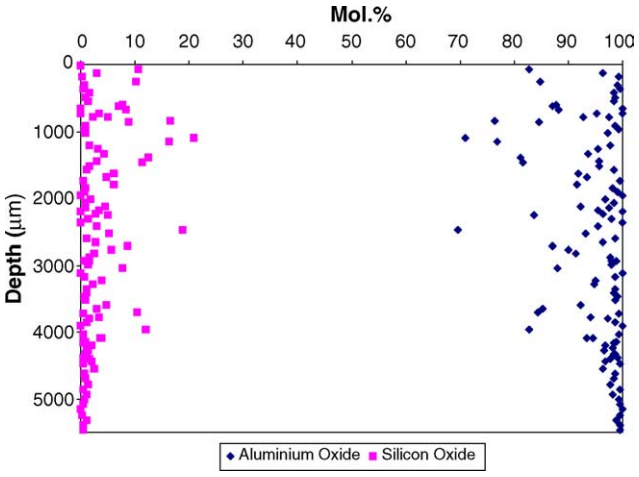

Fig. 11. EDS analysis of the "Powder" FGM heat-treated at 1600 °C for 4 h.

4. Discussion

This work focuses on two alternative fabrication techniques and highlights that different treatments may lead to different FGM microstructures. The most striking difference is that in the "Bulk" FGMs the superficial layer of superabundant glass breaks off from the substrate; on the contrary, the "Powder" FGMs do not experience any delamination but exhibit a remarkable deformation, especially the specimens heat-treated at 1600 °C. Moreover, the superabundant glass in the "Powder" samples undergoes a wide crystallization, which results in a superficial coating rich in zirconia.

During the fabrication process, the glass separates some zirconium oxide, which precipitates in the form of monoclinic zirconia. The zirconium oxide crystallization is more abundant in the "Powder" FGMs than in the "Bulk" ones, since the crystallization kinetics is higher for the powder glass than for the bulk. The glass, which is now poorer in zirconium oxide, gives rise to the crystallization of anorthite. Since the glass composition does not contain any aluminium, the appearance of the anorthite, which is a calcium aluminium silicate, demonstrates that some alumina migrates from the substrate into the glass. This means that a two-way penetration is taking place: while the glass percolates into the polycrystalline alumina, some alumina penetrates into the glass. The anorthite crystallization is likely to be enhanced by the alumina grain boundaries, acting as nucleating agents. As a matter of fact, in the "Bulk" FGM samples the anorthite crystals are widely diffused on the glass–substrate interface, but they are not present on the glass–air interface. In the "Powder" FGMs, instead, the anorthite crystallization involves also the glass–air interface, due to the high reactivity of the glass powder, which is characterized by a wider specific surface than the glass bulk.

The anorthite crystallization may significantly influence the glass depths of penetration. In the samples heat-treated at 1500 °C, the anorthite crystals, which are growing preferentially at the glass–substrate interface, are likely to interfere with the glass penetration, slowing it down. As a consequence, the depth of penetration is much lower in the FGM samples treated at 1500 °C than in the samples treated at 1600 °C. Moreover the crystallization kinetics is quicker for the glass powder than for the bulk and therefore, times being equal, the anorthite is more abundant in the "Powder" FGMs than in the "Bulk" FGMs, while the depth reached by the glass is lower. The anorthite, however, completely melts at 1550 °C and does not hinder the glass penetration at 1600 °C. As a matter of fact, times being equal, the depths of penetration at 1600 °C are quite similar in the "Bulk" FGMs and in the "Powder" FGMs. Indeed the depth reached by the glass after 4 h at 1600 °C is higher in the "Powder" FGMs than in the "Bulk" FGMs, owing to the enhanced kinetics of the glass powder. The anorthite crystallises again while the sample is cooling down, thus giving rise to the crystal formations which can be seen also in the samples treated at 1600 °C.

In order to explain the sample deformation, it should be noted that the glass penetration into the polycrystalline alumina involves two mechanisms[16]:

- After relatively short heat treatments, the glass migrates into the alumina grain junctions, causing a slight volume increase;
- After longer heat treatments, the glass percolates into the alumina grain boundaries, giving rise to a more considerable volume increase.

The second mechanism, which is the main cause of the volume increase, is more active at 1600 °C than at 1500 °C; moreover, its consequences are more relevant after longer treatments. In other words, the second type of glass penetration is scarcely active if the maximum temperature reached is 1500 °C; instead it becomes predominant in the samples treated at 1600 °C and the volume affected is greater after 4 h than after 2 h. Moreover, it should be remarked that the "Powder" FGM samples are much more deformed than the

correspondent "Bulk" ones, since the glass powder is more reactive than the glass bulk, thus enhancing the penetration kinetics. One more reason of the sample deformation may be the alumina grain growth, which is caused by the long stay at high temperature.[11] Finally the deformation of the FGMs samples may be also due to the mismatch in the coefficients of thermal expansion of glass and alumina on one hand and anorthite[17] on the other. The thermodilatometric incompatibility may lead to concentrated thermal residual stresses and local damages, which culminate in the delamination of the "Bulk" FGMs.

When the FGM substrate is considered, some zirconia precipitates can be seen using the SEM. Nevertheless, according to the X-ray diffraction analysis, if the eventual superabundant glass is not considered, the only crystal phase which can be identified in the FGM cross-section is the α-alumina. This means that the amount of the zirconium oxide crystals is so low that it does not reach the diffractometer threshold of detectability. In brief, during the heat treatment the glass penetrates into the alumina, without inducing any chemical reaction or relevant crystallization inside the substrate.

As it may be expected, the depth of penetration depends not only on the crystallization phenomena, but also on the time and temperature of the scheduled heat treatment. Actually, since the sintered alumina is characterized by some residual porosity—about 4.6 vol.%[11]—it may be assumed that the driving force for penetration is capillarity[17] and the depth-time dependence may be expressed by the equation[18]:

$$L = Kt^{1/2}, \qquad K = \sqrt{\frac{r}{2}\frac{\cos\theta}{\eta}\gamma}$$

where L is the glass penetration depth, t is time, K is the coefficient of penetration, r is the capillary radius (assimilated to the alumina pores), θ is the contact angle, γ is the glass surface tension, η is the glass viscosity.

Since at 1600 °C the viscosity of glass is lower[19] and its superficial tension is higher[19] than at 1500 °C, the glass penetration is easier and quicker.

5. Conclusions

Glass–alumina functionally graded materials are new, interesting engineered materials, which can be easily produced by means of glass percolation into a polycrystalline alumina substrate. The described fabrication procedure represents a relatively easy method to fabricate glass–alumina functionally graded materials, since the glass penetration into the alumina substrate leads to a gradual change in composition as a function of depth. However, the fabrication conditions, as well as the initial glass form—powder or bulk—may deeply influence the final FGM microstructure as well as the depth of penetration reached by the glass. The depth of penetration increases with time and temperature. In this study, a glass belonging to the $CaO–ZrO_2–SiO_2$ system was chosen due to its good thermo-mechanical properties. Yet the fabrication heat-treatment induces the crystallization of the superficial superabundant glass, leading to the delamination of the glass top layer in the "Bulk" FGM samples and to the formation of a glass–ceramics coating in the "Powder" FGM samples. Therefore, if the glass–alumina functionally graded materials are intended for an industrial application, it would be recommendable to use the glass in the form of powder and to perform a thermal treatment at 1500 °C for 4 h. As a matter of fact, the reached depth of penetration is appreciable (≈1500 μm) and the sample deformation is negligible, while the superficial glass results in a glass–ceramics coating which adheres well to the substrate.

In conclusion, this work shows that it is possible to engineer the final FGM microstructure by properly setting out the processing parameters. On the other hand, a microstructure-based computational model could define the relation between microstructural details and final properties, thus enabling the complete FGM design, from processing to application. The development of a computational model for overall properties prediction is the focus of current research.

Acknowledgement

The authors would like to express their gratefulness to Eng. Daniele Baldini, who contributed to the preparation and characterization of the ingredient materials and the functionally graded materials.

References

1. Miyamoto, Y., Kaysser, W. A., Rabin, B. H., Kawasaki, A. and Ford, R. G., Functionally graded materials. *Design, Processing and Applications*. Kluwer Academic Publishers, 1999.
2. Mortensen, A. and Suresh, S., Functionally graded metals and metal-ceramic composites. I. Processing. *Int. Mater. Rev.*, 1995, **40**(6), 239–265.
3. Mortensen, A. and Suresh, S., Functionally graded metals and metal-ceramic composites. II. Thermomechanical behaviour. *Int. Mater. Rev.*, 1997, **42**(3), 85–116.
4. Jitcharoen, J., Padture, N. P., Giannakopoulos, A. E. and Suresh, S., Hertzian-crack suppression in ceramics with elastic-modulus-graded surfaces. *J. Am. Ceram. Soc.*, 1998, **81**(9), 2301–2308.
5. Suresh, S., Ollson, M., Giannakopoulos, A. E., Padture, N. P. and Jitcharoen, J., Engineering the resistance to sliding-contact damage through controlled gradients in elastic properties at contact surfaces. *Acta Mater.*, 1999, **47**(14), 3915–3926.
6. Cannillo, V., Manfredini, T., Corradi, A. and Carter, W., Numerical models of the effect of heterogeneity on the behavior of graded materials. *Key Eng. Mater.*, 2002, **206–213**, 2163–2166.
7. Cannillo, V. and Carter, W. C., Numerical models of the effect of elastic heterogeneity on the toughness of graded materials. In *Advances in Fracture Research, Proceedings of ICF10*, eds. K. Ravi-Chandar, B. L. Karihaloo, T. Kishi, R. O. Ritchie, A. T. Yokobori Jr. and T. Yokobori., 2001.
8. Leonelli, C. and Siligardi, C., $CaO-SiO_2-ZrO_2$ glasses: modelling and experimental approach. *Recent Res. Dev. Mater. Sci.*, 2002, **3**, 599–618.

9. Ming, D., Pei, G., Maewal, A. and Asaro, R. J., A micromechanical study of residual stresses in functionally graded materials. *Acta Mater.*, 1997, **45**(8), 3265–3276.
10. FN S.p.A. Nuove tecnologie e Servizi Avanzati, Bosco Marengo, AL, Italy.
11. Cannillo, V., Manfredini, T., Montorsi, M., Siligardi, C. and Sola, A., Glass–alumina functionally graded materials preparation and compositional profile evaluation, submitted for publication.
12. Siligardi, C., D'Arrigo, M. C., Leonelli, C. and Pellacani, G. C., Bulk crystallization of glasses belonging to the calcia-zirconia-silica system by microwave energy. *J. Am. Ceram. Soc.*, 2000, **83**(4), 1001–1003.
13. Quinn, G. D., Patel, P. J. and Lloyd, I., Effect of loading rate upon conventional ceramic microindentation hardness. *J. Res. Nat. Inst. Stand. Technol.*, 2002, **107**(3), 299–306.
14. Ponton, C. B. and Rawlings, R. D., Vickers indentation fracture test. Part 1. Review of literature formulation of standardised indentation toughness equations. *Mater. Sci. Technol.*, 1989, **5**, 865–871.
15. Ponton, C. B. and Rawlings, R. D., Vickers indentation fracture test. Part 2. Application and critical evaluation of standardised indentation toughness equations. *Mater. Sci. Technol.*, 1989, **5**, 961–970.
16. Flaitz, P. L. and Pask, J. A., Penetration of polycristalline alumina by glass at high temperatures. *J. Am. Ceram. Soc.*, 1987, **70**(7), 449–455.
17. Strnad, Z., Glass ceramic materials. *Glass Ceramic Science and Technology*, *8*. Elsevier, 1986.
18. Kuromitsu, T., Yoshida, H., Takebe, H. and Morinaga, K., Interaction between alumina and binary glasses. *J. Am. Ceram. Soc.*, 1997, **80**(6), 1583–1587.
19. Navarro, J. M. F., *El Vidrio*. C.S.I.C, Madrid, 1991.